JOURNAL OF THERMOPHYSICS AND HEAT TRANSFER
Vol. 7, No. 4, Oct.–Dec. 1993

Measurements of Laminar Mixed Convection Flow over a Horizontal Forward-Facing Step

H. I. Abu-Mulaweh,* B. F. Armaly,† and T. S. Chen‡
University of Missouri—Rolla, Rolla, Missouri 65401

Measurements and predictions of buoyancy-assisting laminar mixed convection flow over a horizontal, two-dimensional forward-facing step are reported. Laser-Doppler velocimeter (LDV) and cold wire anemometer were used to simultaneously measure the velocity and the temperature distributions, respectively. Flow visualizations were conducted to determine the reattachment lengths for different inlet velocities (0.255 m/s $\leq u_0 \leq$ 0.50 m/s), wall freestream temperature differences (0°C $\leq \Delta T \leq$ 37°C) and step heights (0.79 cm $\leq s \leq$ 1.75 cm). The results reveal that the buoyancy force due to wall heating has a negligible effect on the velocity and temperature distributions and the reattachment lengths, as long as the flow remains stable and two-dimensional (i.e., prior to the onset of vortex instability on the heated wall). The inlet velocity and the step height, on the other hand, significantly affect the flow and thermal fields. The local heat transfer coefficient is found to increase as the inlet velocity increases and the step height decreases. On the other hand, the length of the recirculation regions upstream and downstream of the step are found to increase as the inlet velocity and the step height increase (i.e., with increasing Reynolds number). Correlation equations are developed to predict the reattachment lengths that appear upstream and downstream of the step. The measured results agree well with numerical predictions.

Nomenclature

Gr_s = Grashof number, $g\beta(T_w - T_\infty)s^3/\nu^2$
g = gravitational acceleration
H = height of computational domain at inlet section
h = heat transfer coefficient, $-k(\partial T/\partial y)_{y=0}/(T_w - T_\infty)$
k = thermal conductivity
Nu_s = local Nusselt number, hs/k
p = pressure
Pr = Prandtl number, ν/α
Re_s = Reynolds number, $u_0 s/\nu$
s = step height
T = fluid temperature
T_w = heated wall temperature
T_∞ = freestream temperature
U = dimensionless streamwise velocity component, u/u_0
u = streamwise velocity component
u_0 = inlet velocity
u_∞ = local freestream velocity
V = dimensionless transverse velocity component, v/u_0
v = transverse velocity component
X, Y = dimensionless streamwise and transverse coordinates, x/s, y/s
X_e, X_i, X_r, X_s = x_e/s, x_i/s, x_r/s, x_s/s
x, y = streamwise and transverse coordinates measured from the upper corner of the step
x_e = downstream heated length
x_i = inlet length upstream of the step
x_r = reattachment length of the recirculation region downstream of the step
x_s = length of the recirculation region upstream of the step
α = thermal diffusivity
β = volumetric thermal expansion coefficient
ΔT = temperature difference, $T_w - T_\infty$
δ_s = boundary-layer thickness at the step, $5x_i/Re_{xi}^{1/2}$
θ = dimensionless temperature, $(T - T_\infty)/(T_w - T_\infty)$
ν = kinematic viscosity
ρ = density

Received July 24, 1992; revision received Dec. 28, 1992; accepted for publication Dec. 28, 1992. Copyright © 1993 by the American Institute of Aeronautics and Astronautics, Inc. All rights reserved.

*Lecturer in Mechanical Engineering, Department of Mechanical and Aerospace Engineering and Engineering Mechanics.

†Professor of Mechanical Engineering, Department of Mechanical and Aerospace Engineering and Engineering Mechanics. Member AIAA.

‡Curator's Professor of Mechanical Engineering, Department of Mechanical and Aerospace Engineering and Engineering Mechanics. Associate Fellow AIAA.

Introduction

IN many flows of practical interest the existence of flow separation and recirculation regions due to a sudden compression in flow geometry plays an important role in the design of heat transfer devices, such as high-performance heat exhangers, cooling systems for electronic equipments, cooling passages of turbine blades, combustion chambers, and chemical process equipments. For a two-dimensional flow past a forward-facing step, one or two separated flow regions may develop adjacent to the step, depending upon the magnitude of the flow Reynolds number and the thickness of the momentum boundary layer at the step. A recirculation region can develop upstream of the step and another recirculation region can develop downstream of the step. These separated flow regions make this geometry more complicated to study than the backward-facing step in which only one separated flow region occurs behind the step. Owing to this fact, the backward-facing step geometry has been studied extensively, but little attention has been given to the flow past a forward-facing step. The numerical investigations of Fletcher and Srinivas[1] and Baron et al.[2] are the only studies which could be found in the open literature that specifically examined flow past a forward-facing step. The flow over a blunt flat plate and over a rib will exhibit some of the general behaviors as the forward-facing step geometry. Lane and Loehrke[3] experimentally examined the fluid flow aspect, Zelenka and Loehrke[4]

performed some heat transfer measurements of laminar flow over a blunt flat plate, and Hsieh and Huang[5,6] and Hsieh et al.[7] examined the flow over a rib. In these cases the focus was on the forced convection regime.

In the present study, consideration is given to mixed convection buoyancy-assisting, two-dimensional, laminar boundary-layer airflow over a horizontal forward-facing step. The step and the wall downstream of the step is maintained at a uniform temperature while the upstream wall is adiabatic. Results of interest, such as temperature and velocity distributions, local Nusselt numbers, and reattachment lengths are reported to illustrate the effects of the buoyancy force (i.e., wall temperature), thickness of the approaching momentum boundary layer at the step, and the flow Reynolds number on these parameters.

Experimental Apparatus and Procedure

The experimental study was performed in an existing low-turbulence, open-circuit air tunnel. Details of the air tunnel have been described by Ramachandran et al.[8] and a schematic is shown in Fig. 1. The test section of the tunnel consisted of a heated forward-facing step geometry, with an adiabatic upstream section (20.0-cm long and 30.48-cm wide), a heated (constant temperature) forward-facing step and downstream section (79-cm long and 30.48-cm wide) behind the step. The test section is instrumented with laser-Doppler velocimeter and cold wire anemometer to measure the velocity and temperature distributions as described by Baek et al.[9] The heated wall, downstream of the step, was constructed of four layers which were held together by screws and instrumented to provide an isothermal heated surface. The upper layer was an aluminum plate (1.27-cm thick) instrumented with 18 copper-constantan thermocouples that were distributed in both the axial and the transverse directions. Each thermocouple was inserted into a hole on the backside of the plate and its measuring junction was flush with the test surface. The second layer consisted of five separately controlled heater pads, and an insulation layer formed the third layer. The bottom layer was an aluminum plate which served as backing and support for the structure of the plate. The front edge of this heated plate was squared to form the heated forward-facing step. The upstream section of the forward-facing step was constructed from Plexiglas® which was simulated as adiabatic surface. Minimum contact was achieved between the upstream plate and the step by chamfering the Plexiglas surface, thus minimizing the heat transfer between the two surfaces. The height of the step could be changed to any desired value (0.79–1.75 cm). The inlet velocity in the tunnel could be varied between 0.25–3.0 m/s and the heated downstream plate could be maintained at a uniform and constant temperature between 25–75°C by controlling power input to the individual heaters.

Flow visualizations were conducted, by utilizing a 15-W collimated white light beam, 2.5 cm in diameter, to examine

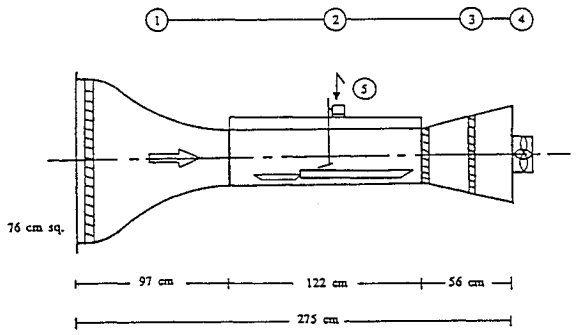

1. Mixing Chamber 2. Test Section 3. Diffuser
4. Fan Assembly 5. Probe Traversing Unit

Fig. 1 Schematic of air tunnel.

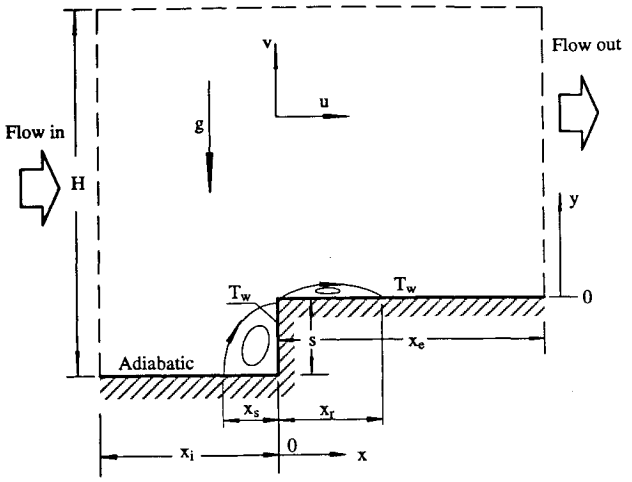

Fig. 2 Schematic diagram of the calculation domain.

the flow and to detect the reattachment length. The flow was seeded with Glycerin particles, 2–5 μ in diameter, which served as scattering centers for flow visualization and for LDV measurements.

Numerical Analysis

The experimental geometry and boundary conditions were modeled for numerical simulation, as shown schematically in Fig. 2. The lengths x_i, x_s, x_r, x_e, s, and H are not presented to the same scale in Fig. 2. These lengths are selected for clarity. The upstream and downstream recirculation regions are shown schematically on this figure. The upstream wall was considered as adiabatic, while the wall downstream of the step and the step itself were considered as being heated to a uniform temperature T_w. The gravitational acceleration g is acting vertically downward. The thermal properties were considered to be constant but evaluated at the film temperature $T_f = (T_w + T_\infty)/2$.

By utilizing the Boussinesq approximation ($\beta\Delta T < 0.1$ in this experiment), the governing conservation equations for the physical problem under consideration can be written as follows:

$$\frac{\partial U}{\partial X} + \frac{\partial V}{\partial Y} = 0 \tag{1}$$

$$U\frac{\partial U}{\partial X} + V\frac{\partial U}{\partial Y} = -\frac{\partial P}{\partial X} + \left(\frac{1}{Re_s}\right)\left(\frac{\partial^2 U}{\partial X^2} + \frac{\partial^2 U}{\partial Y^2}\right) \tag{2}$$

$$U\frac{\partial V}{\partial X} + V\frac{\partial V}{\partial Y} = -\frac{\partial P}{\partial Y} + \left(\frac{1}{Re_s}\right)\left(\frac{\partial^2 V}{\partial X^2} + \frac{\partial^2 V}{\partial Y^2}\right) + \left(\frac{Gr_s}{Re_s^2}\right)\theta \tag{3}$$

$$U\frac{\partial \theta}{\partial X} + V\frac{\partial \theta}{\partial Y} = \left(\frac{1}{PrRe_s}\right)\left(\frac{\partial^2 \theta}{\partial X^2} + \frac{\partial^2 \theta}{\partial Y^2}\right) \tag{4}$$

The boundary conditions are given by

$$-1 < Y < \left(\frac{H}{s}\right) - 1, \quad X = -X_i: \quad \text{(at inlet)}$$

$$U = 1, \quad V = \theta = 0 \tag{5}$$

$$1 < Y < \left(\frac{H}{s}\right) - 1, \quad X = X_e: \quad \text{(at exit)}$$

$$\frac{\partial^2 U}{\partial X^2} = \frac{\partial^2 V}{\partial X^2} = \frac{\partial^2 \theta}{\partial X^2} = 0 \tag{6}$$

$$Y = \left(\frac{H}{s}\right) - 1, \quad -X_i < X < X_e: \quad \text{(upper wall)}$$

$$U = V = \theta = 0 \tag{7}$$

$$Y = -1, \quad -X_i < X < 0: \quad \text{(upstream wall)}$$

$$U = V = 0, \quad \frac{\partial \theta}{\partial Y} = 0 \tag{8}$$

$$-1 < Y < 0, \quad X = 0: \quad \text{(step wall)}$$

$$U = V = 0, \quad \theta = 1 \tag{9}$$

$$Y = 0, \quad 0 < X < X_e: \quad \text{(downstream wall)}$$

$$U = V = 0, \quad \theta = 1 \tag{10}$$

The x_i, x_e, H, and s values were taken as 20, 40, 16, and 0.79–1.75 cm, respectively. The governing set of coupled partial differential equations was solved by using a finite-difference scheme using the SIMPLE algorithm, as described by Patankar.[10] The solution procedure starts with the initial estimates for velocities, temperatures, and pressure fields, along with the physical boundary conditions, and an iteration is performed until a converged solution is obtained. The momentum equations are employed first in the iteration process, using the estimated temperature for the buoyancy force calculations, and the energy equation is then solved to upgrade the temperature. This process is repeated for each iteration step until a converged solution is obtained. Convergence of the solution is considered satisfactory when the normalized sum of residuals (mass, momentum, and energy) over the whole calculation domain was less than 0.01.

A nonuniform grid distribution was used in the computations, in both the streamwise and the transverse coordinates. A large number of grid points were used adjacent to the walls in the y-coordinate direction, and near the step and the reattachment point in the x-coordinate direction, where large variations of velocities were detected from measurements. Solutions were performed with different grid densities and grid numbers to ensure a grid-independent solution. A grid density of $N_x \times N_y = 100 \times 80$ was found to be sufficient in providing a grid-independent solution. For two mesh sizes of 100×80 and 140×120, the maximum changes in the predicted velocity, Nusselt number, and reattachment length were less than 3, 1.5, and 1%, respectively. The computations were performed on an Apollo 10000 computer and required 1000–1500 iterations in most cases to reach a converged solution.

Results and Discussion

The uniformity and the two-dimensional nature of the flow was verified through flow visualizations and through measurements of velocity and temperature across the width of the air tunnel, at various heights above the test surface. These measurements displayed a wide region, about 80%, around the center of the tunnel's width where the flow can be approximated (to within 5%) as being two-dimensional. All reported streamwise velocity and temperature distributions in the transverse (y) direction were taken along the midplane ($z = 0$) of the plate's width, and only after the system had reached steady-state conditions.

Measurements of velocity distributions were carried out in both regions upstream and downstream of the step. On the other hand, measurements of temperature distributions were carried out only in the region downstream of the step because the upstream wall was kept adiabatic. For the case of $s = 1.27$ cm, inlet velocity $u_0 = 0.485$ m/s, and temperature difference $(T_w - T_\infty) = 7.5$°C, the measured and the predicted velocity and temperature distributions are presented in Figs. 3 and 4, for the regions upstream and downstream of the step, respectively. It is noted that in these figures, u is normalized by u_∞ at the edge of the boundary layer. Figure 3 shows clearly that negative velocities exist only in the velocity distribution at $X = -0.787$, indicating that this location lies inside the recirculation region that develops in front, or upstream, of the step (as shown schematically in Fig. 2). The other velocity distributions at $X = -2.362$ and -4.724 are outside this recirculation region. Similarly, the velocity distribution at $X = 0.787$, in Fig. 4, exhibits some negative velocities, indicating that this distribution is located in the recirculation region that develops behind, or downstream, of the step (as shown schematically in Fig. 2). Figure 4 clearly shows that the recirculation region that develops downstream of the step is very shallow. It also shows that the temperature gradient at the heated wall decreases as the streamwise distance from the forward-facing step increases. As can be seen from these two figures, good agreement exists between the measured and the predicted results (within 5%).

Similar to the horizontal flat plate geometry and the horizontal backward-facing step geometry, vortex instabilities start to develop adjacent to the horizontal heated wall in this geometry at high heating levels. This development limits the applicability of the two-dimensional laminar flow solution for

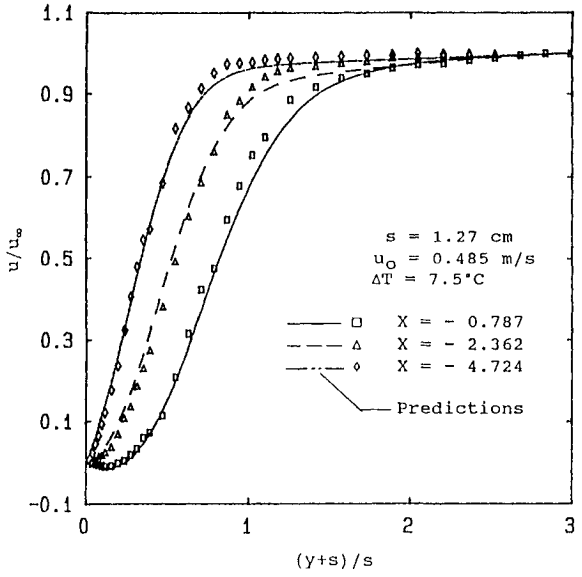

Fig. 3 Dimensionless axial velocity distributions upstream of the step (uncertainty in u/u_∞ is ±0.014, and in y/s is ±0.022).

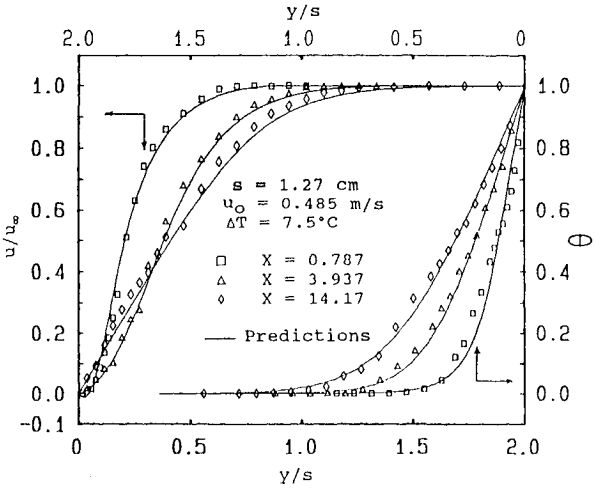

Fig. 4 Dimensionless axial velocity and temperature distributions downstream of the step (uncertainty in u/u_∞ is ±0.014, in θ is ±0.025, and in y/s is ±0.022).

predicting the flow and thermal fields characteristics in this geometry. Due to this fact, all the measurements reported in this study were performed in the region where the flow is stable and two-dimensional. Figure 5 illustrates the effect of buoyancy forces (i.e., heating the downstream wall) on the velocity and temperature distributions for the case of $s = 1.27$ cm, $u_0 = 0.485$ m/s, and four different temperature differences $\Delta T = 0$, 7.5, 23, and 37°C at a downstream location $X = 3.937$. It can be seen from the figure that the wall heating has a negligible effect on the streamwise velocity and temperature distributions as long as the flow remains stable and two-dimensional (i.e., prior to the onset of vortex instability). This is due to the fact that the buoyancy force component in the streamwise direction is zero.

Figure 6 illustrates the effects of inlet velocity ($u_0 = 0.3$ and 0.5 m/s) on the axial variation of the local Nusselt number for the case of $s = 0.79$ cm and $\Delta T = 7.5$°C. The Nusselt number has its largest value at the upper corner of the step (not shown in the figure). For a given inlet velocity the local Nusselt number decreases rapidly from its largest value and then starts to level off to a constant value. Also, it can be seen that the local Nusselt number is higher for higher inlet velocities. The measured results agree favorably well with numerical predictions (within 8%).

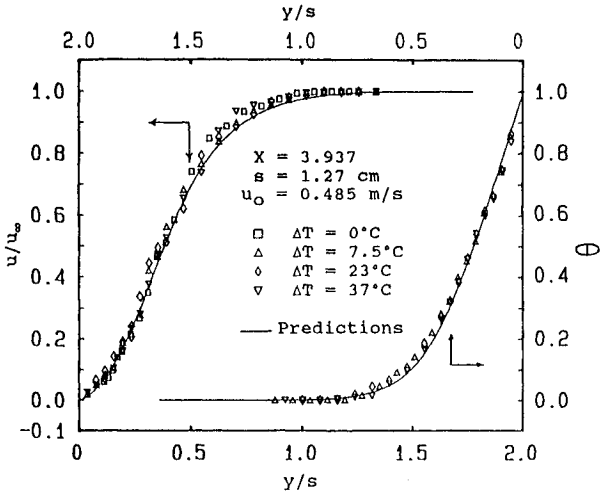

Fig. 5 Effects of wall temperature on the velocity and temperature distributions (uncertainty in u/u_∞ is ±0.014, in θ is ±0.025, and in y/s is ±0.022).

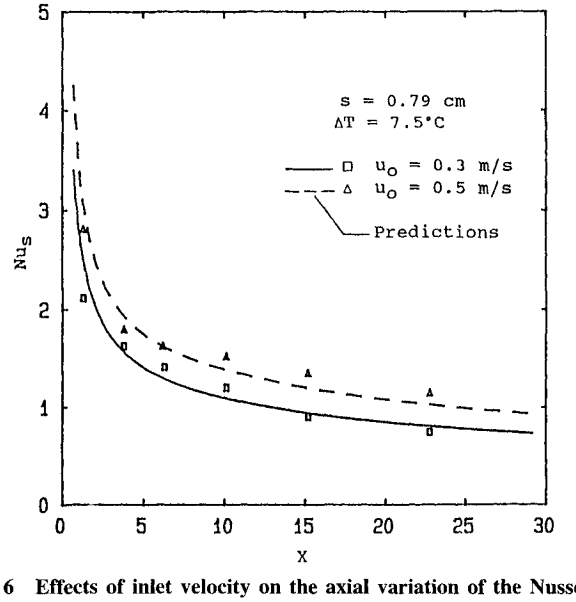

Fig. 6 Effects of inlet velocity on the axial variation of the Nusselt number (uncertainty in Nu_s is ±0.05 and in X is ±0.05).

The effects of the step height ($s = 0.79$, 1.27, and 1.75 cm) on the rate of convective heat transfer from the heated wall downstream of the step are illustrated in Fig. 7 for the case of $u_0 = 0.485$ m/s and $\Delta T = 7.5$°C. The figure shows that the convective heat transfer coefficient h increases as the step height decreases. This is due to the fact that the length of the upper recirculation region decreases as the step height decreases, as was discussed earlier. For comparison, the flat plate convective heat transfer coefficient is also plotted on this figure. It can be seen that the flat plate results, near the step, are higher than the results of the forward step geometry. The relatively lower velocities that develop in the recirculation region adjacent to the heated wall is responsible for decreasing the heat transfer coefficient in that region. The corresponding Nu_s values are also presented in this figure. It is seen that the effect of the step height on the Nusselt number is opposite to its effect on the convective heat transfer coefficient, i.e., Nusselt number increases as the step height decreases. This is caused by the definition of the Nusselt number ($Nu_s = hs/k$) in this study. The figure also shows that the deviations between the experimental and predicted Nusselt numbers are smaller than those of the heat transfer coefficient. This is due to the fact that the Nusselt number is deduced by multiplying the heat transfer coefficient by s/k (a positive fraction, less than one in this study), thus resulting in a smaller deviation.

Flow visualization studies were also conducted to determine the effects of step height, inlet velocity, and wall freestream temperature difference on the reattachment length downstream of the step (upper recirculation region) and the length of the recirculation region upstream of the step (lower region). It was observed that one or two recirculation regions may develop, depending upon the step height and the thickness of the approaching momentum boundary layer at the step. In this study it was determined that when $\delta_s/s > 1.15$, the upper recirculation region (downstream of the step) disappears and only one recirculation region (upstream of the step) exists in front of the step. When $\delta_s/s < 0.7$ transition from laminar flow to turbulent flow starts in the upper recirculation region (downstream of the step). As stated earlier, the buoyancy force resulting from the wall heating essentially does not affect the lengths of the recirculation regions, as long as the flow remains stable and two-dimensional. The measured and the numerically predicted reattachment lengths compared favorably well (within 4%). The measured reattachment length of

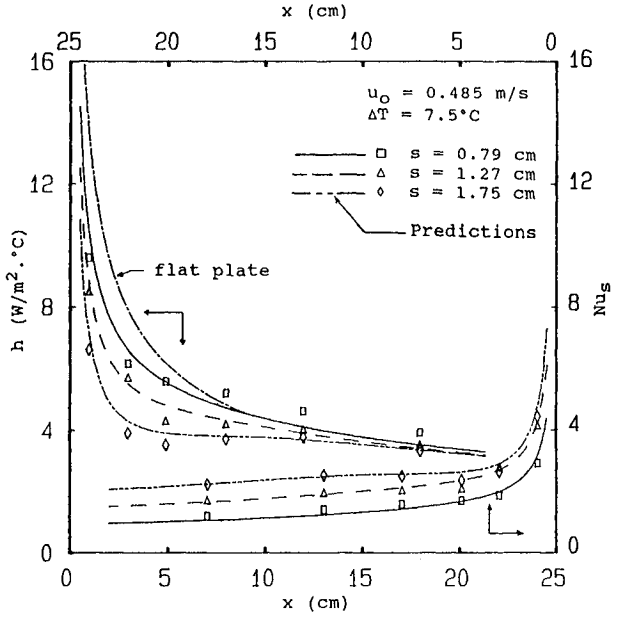

Fig. 7 Effects of step height on the convective heat transfer coefficient and the Nusselt number (uncertainty in h is ±0.04 W/m²·°C, and in Nu_s is ±0.05).

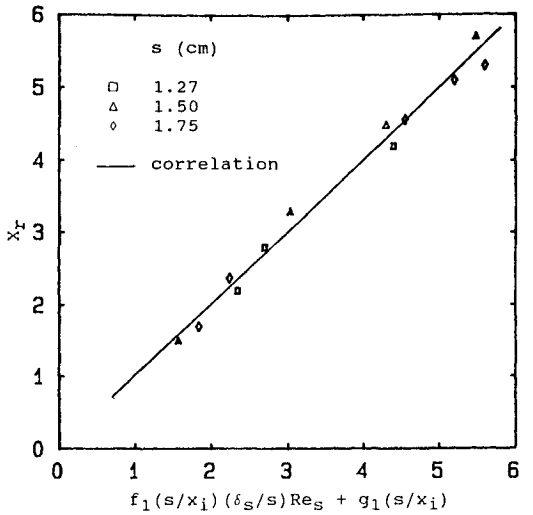

Fig. 8 Correlation for the reattachment length of the upper recirculation region (downstream of the step) (uncertainty in X_r is ±0.25).

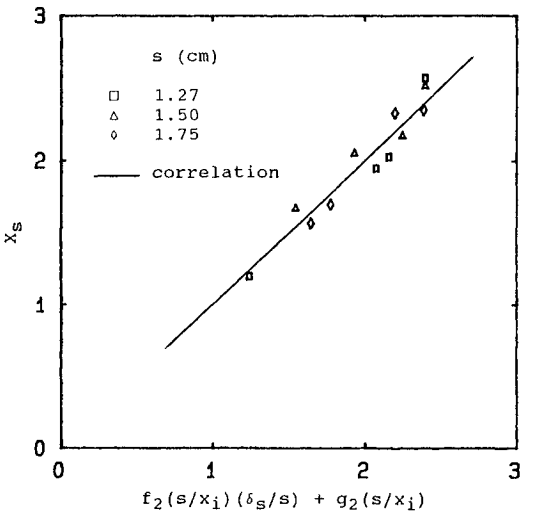

Fig. 9 Correlation for the separation length of the upstream recirculation region (in front of the step) (uncertainty in X_s is ±0.25).

the upper recirculation region (downstream of the step) X_r for different flow conditions and step heights in this study can be correlated in terms of the calculated thickness of the approaching momentum boundary layer at the step δ_s, the step height s, and Re_s (based on the step height) by the following equation:

$$X_r = f_1(s/x_i)(\delta_s/s)Re_s + g_1(s/x_i) \quad (11)$$

where

$$f_1(s/x_i) = 0.3735(s/x_i) + 0.00265 \quad (12)$$

$$g_1(s/x_i) = -23.989(s/x_i) - 6.077 \quad (13)$$

Similarly, the observed lengths of the upstream recirculation region (in front of the step) can be correlated by

$$X_s = f_2(s/x_i)(\delta_s/s) + g_2(s/x_i) \quad (14)$$

where

$$f_2(s/x_i) = 1219.7(s/x_i)^2 - 201.2(s/x_i) + 5.52 \quad (15)$$

$$g_2(s/x_i) = -3.057(s/x_i) + 4.739 \quad (16)$$

The momentum boundary-layer thickness at the step, the step height and the Reynolds number ranges used to develop the above correlations are $1.10 < \delta_s < 1.78$ cm, $1.27 < s < 1.75$ cm, and $270 < Re_s < 570$. The measured results along with the results from the correlation Eqs. (11) and (14), are presented in Figs. 8 and 9, respectively. The empirical Eqs. (11) and (14) predict the measured lengths of the recirculation regions to within 12%. The size of both recirculation regions increases as the freestream velocity or the step height increases.

Conclusions

Measurements were conducted for buoyancy-assisting, laminar mixed convection flow over a horizontal forward-facing step. The results reveal that the inlet velocity and step height (Reynolds number) significantly affect the local heat transfer rate and the size of the recirculation regions. On the other hand, the buoyancy force resulting from the heating of the downstream wall has negligible effect on these parameters, because that buoyany force has no streamwise component. It has been found that the size of the recirculation regions increases, and the heat transfer rate from the heated downstream wall decreases as the step height increases, and that both parameters increase as the inlet velocity increases. Also, one or two recirculation regions may develop adjacent to the step, depending upon the thickness of the approaching momentum boundary layer at the step and the step height. It has also been observed that when $\delta_s/s > 1.15$, the upper recirculation region disappears and only one recirculation region exists upstream of the step, and that when $\delta_s/s < 0.7$ transition from laminar flow to turbulent flow starts to develop in the upper recirculation region downstream of the step.

Acknowledgments

The present study was supported by a Grant from the National Science Foundation (NSF CTS-8923010). Bin Hong assisted in the numerical computations.

References

[1]Fletcher, C. A. J., and Srinivas, K., "Stream Function Vorticity Revisited," *Computer Methods in Applied Mechanics and Engineering*, Vol. 41, No. 3, 1983, pp. 297–322.

[2]Baron, A., Tsou, F. K., and Aung, W., "Flow Field and Heat Transfer Associated with Laminar Flow over a Forward-Facing Step," *Proceedings of the 8th International Heat Transfer Conf.*, Hemisphere, Washington, DC, Vol. 3, 1986, pp. 1077–1082.

[3]Lane, J. C., and Loehrke, R. I., "Leading Edge Separation from a Blunt Plate at Low Reynolds Number," *Journal of Fluid Engineering*, Vol. 102, Dec. 1980, pp. 494–496.

[4]Zelenka, R. L., and Loehrke, R. I., "Heat Transfer from Interrupted Plates," *Journal of Heat Transfer*, Vol. 105, No. 1, 1983, pp. 172–177.

[5]Hsieh, S. S., and Huang, D. Y., "Flow Characteristics of Laminar Separation on Surface-Mounted Ribs," *AIAA Journal*, Vol. 25, No. 6, 1987, pp. 819–823.

[6]Hsieh, S. S., and Huang, D. Y., "Numerical Computation of Laminar Separated Forced Convection on Surface-Mounted Ribs," *Numerical Heat Transfer*, Vol. 12, No. 3, 1987, pp. 335–348.

[7]Hsieh, S. S., Shih, H. J., and Hong, Y. J., "Laminar Forced Convection from Surface-Mounted Ribs," *International Journal of Heat and Mass Transfer*, Vol. 33, No. 9, 1990, pp. 1987–1999.

[8]Ramachandran, N., Armaly, B. F., and Chen, T. S., "Measurements and Predictions of Laminar Mixed Convection Flow Adjacent to a Vertical Surface," *Journal of Heat Transfer*, Vol. 107, No. 3, 1985, pp. 636–641.

[9]Baek, B. J., Armaly, B. F., and Chen, T. S., "Measurements in Buoyancy-Assisting Separated Flow Behind a Vertical Backward-Facing Step," *Journal of Heat Transfer* (to be published).

[10]Patankar, S. V., *Numerical Heat Transfer and Fluid Flow*, Hemisphere, Washington, DC, 1980.